

Use of chitosan impregnated modified bentonite as an adsorbent for remediation of oil spill from aqueous solution

Zena Waheed Thany¹*, Ali Mousa Ridha¹

¹ Department of Materials Engineering Technology, Engineering Technical College– Baghdad, Middle Technical University, Baghdad, Iraq

*Corresponding author E-mail:

Abstract

The focus of this work was to study the removal of oil spill from aqueous solution by adsorption onto different adsorbents such as raw bentonite (RB), modified bentonite (MB), chitosan-modified Bentonite (CS-MB10) and Chitosan-modified Bentonite (CS-MB30). The CS-MB10 and CS-MB30 were prepared by loading biopolymer Chitosan onto modified bentonite with different amounts of chitosan as 10 wt.% and 30 wt.% respectively. The modified bentonite was made by exchanging Cetyltrimethylammonium bromide (CTAB) with calcium ions in the Iraqi bentonite structure. All adsorbents were characterized by FTIR, surface area and pore volume. The maximum adsorption efficiency of oil at 1.4g was found to be 72.46% for RB, 89.09% for MB, and at 1.2g were found to be 90.81% for CS-MB10 and 95.85% for CS-MB30. Best contact time and pH were selected at 2 h and pH 6 with the maximum adsorption efficiency of oil onto each of RB, MB, CS-MB10 and CS-MB30. The Temkin isotherm gave a better fit to the experimental data than Langmuir and Freundlich adsorption isotherm for oil removal onto CS-MB10 and RB and the Langmuir isotherm gave a better fit to the experimental data than Temkin and Freundlich adsorption isotherm for oil onto CS-MB30 and MB.

Keywords: Adsorption; Oil Removal; Chitosan Impregnated Bentonite; Bentonite; Chitosan.

1. Introduction

In recent years there has been a growing concern about the danger of some industrial fields, such as food processing, transportation and petroleum refining and petrochemical. These activities produce large amounts of oily wastewater that may be discharged into surface water without suitable treatment. Then, this problem can cause a serious threat to the environment and the human health. Oily wastewater contains many types of toxic materials like phenols, polyaromatic hydrocarbons, and petroleum hydrocarbons. These toxic materials are a threat to the growth of plant and creature, and furthermore mutagenic and carcinogenic to individual. Subsequently, the concentration of these materials must be treated to an acceptable level before discharging it into the environment [1]. Other important sources of oily sewage are the crude oil, fuel treatment process and effluent from gas turbine stations [2].

At present, many types of treatment methods used to remove oil from water: mechanical, physicochemical, chemical, and biochemical treatments [2]. Conventional approaches to remove oil pollution have included gravity detachment and skimming, broke down air buoyancy, de-emulsification, coagulation, and flocculation. Gravity division took after by skimming is proficiency to expel free oil from wastewater. The oil - water separator is widely used to separate oil from water due to simplicity and the relatively low cost. However, this treatment is not efficient in eliminating minimal oil droplets and emulsions. Sedimentation is usually used to remove the oil that adheres to the surface of solid particles. Oil that adheres to the surface of solid particles. Dissolved Air Flotation (DAF) uses air to increase the buoyancy of smaller oil droplets and to enhance

the separation [3]. However, those treatment technologies are either ineffective or form secondary products. Moreover, they can be highly expensive. Therefore, the choice of the appropriate method does not depend only on the efficiency, but it should rather integrate environmental and economic aspects.

Chitosan has excellent adsorbance capacities, low cost and low efforts compared to others, so it has a great interest for pollutants remediation [4]. So it has a wide range of applications in many industries like wastewater treatment, food, biomedicine, agriculture, textile and paper, biotechnology, cosmetics and others industries.

Bentonite, montmorillonite, sepiolite, smectite and zeolite are the types of clays that considered as an alternative low cost adsorbant. The wide utilization of clays is the consequence of their particular surface area, high mechanical and chemical stability, and assortment of surface and structural properties. The sorption ability of ability is usually determined by pore structure and chemical nature [5].

The overall objective of this work is to use eco-friendly materials such as Chitosan impregnated modified bentonite as a novel adsorbent for the remediation of oil spill from aqueous solution. Using different adsorbents, the effect of the effects of adsorbent dosage, pH value and contact time on the adsorption process of the oil for raw bentonite (RB), modified bentonite (MB), Chitosan impregnated modified bentonite with different amounts of Chitosan (10 wt.% and 30 wt.%) were studied. The equilibrium isotherms Langmuir, Freundlich and Temkin models were investigated.

2. Materials and methods

2.1. Materials

Bentonite

The Iraqi clay mineral, calcium bentonite powder form (Ca-B) was used in this study. It was provided by Iraqi National Company for Geological Survey and Mining, Baghdad. The particle sizes of bentonite is 2-3 mm. The chemical composition of calcium bentonite (Ca-B) provided by the supplier is presented in the Table 1. The molecular formula of bentonite was: $Mg_2Al_3Si_4O_{10}(OH)_2[Na, Ca]$.

Table 1: Chemical Properties of Iraqi Calcium Bentonite (Ca-B)

Materials	Wt.%
SiO ₂	60
Al ₂ O ₃	13.8
H ₂ O	4
Fe ₂ O ₃	3
CaO	2.7
MgO	6
L.O.L	10.5

Chitosan

Deacetylated chitin ($C_6H_{11}NO_4$)_n chips was used in this study as a biopolymer. Low molecular weight (50,000- 190,000 g/mol) Chitosan supplied by Central Drug House (P) Ltd.7/28 Vardaan House, Daryaganj, New Delhi-(INDIA).

Surfactant

Cetyltrimethyl Ammonium Bromide (CTAB) was used in this study as surfactant to modified bentonite.

2.2. Experimental

Figure 1 describes a flow chart of experimental work of removing crude oil from synthetic oily water by using the adsorption technique.

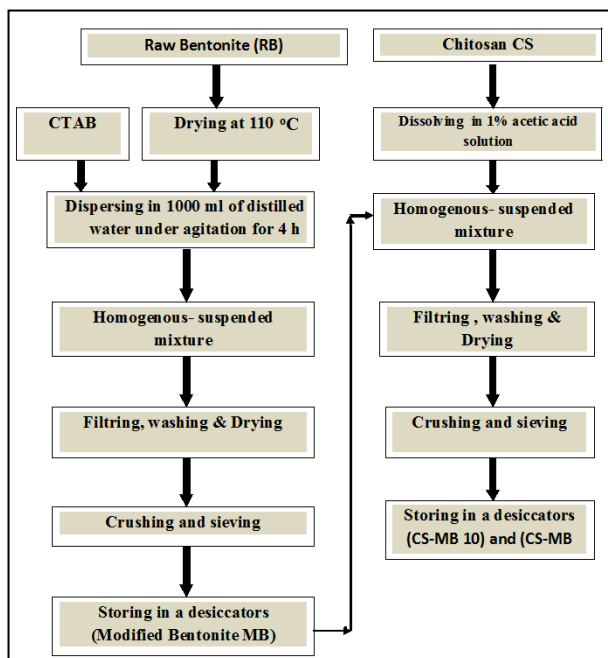


Fig. 1: Flowchart of Chitosan-Modified Bentonite.

2.3. Preparation of adsorbents

a) Raw Bentonite

As received bentonite was ground and sieved through a 2mm mesh and dried at 75°C for 2 hours using drying furnace, Model RWF, Rapid heating chamber-Japan. Then, the dried bentonite that known

as raw bentonite was stored in desiccators for additionally utilize. This is referred to as raw bentonite (RB).

b) Modified Bentonite

100 g of dried bentonite was dispersed in 1000 ml of distilled water under agitation for 4 h to provide homogenous-suspended mixture of bentonite. 20g of cetyltrimethyl ammonium bromide (CTAB) was dissolved by heating the water. It was slowly poured into the bentonite suspension at 70°C for 1h. Then, it was agitated for 24 h without heating. The solution was filtered and washed several times with distill water until it passes free of bromide ions as tested by silver nitrate. Then, the impregnated bentonite was dried at 75°C for 24h. The final product was crushed and sieved into granular with an average size of 2 mm and then kept for further use. This is referred to as modified bentonite (MB). The flow chart of MB preparation process is shown in Figure 2.

c) Impregnation of Chitosan-Modified Bentonite

The impregnation solution of the active component (Chitosan CS) was prepared by dissolving a given amount of chitosan in 1% acetic acid solution. The solution was stirred continuously for 2h by using magnetic stirrer and with maintaining temperature at 25°C. A certain amount of modified bentonite was added into a specific volume of distill water at the ambient temperature. Then chitosan solution was added slowly, step by step, to the mixture of modified bentonite under agitation for 24 h and 60°C. The resulted mixture was filtered and washed in a large amount of distill water to reduce surplus chemicals. Then the filter cake was immersed in 1M of sodium hydroxide solution to precipitate biopolymer Chitosan onto modified-Bentonite. Then, the resulted mixture was filtered and washed with several times of distill water. Then the sample was dried in oven at 75°C for 6h after washing and filtration. Finally the prepared bio-composite adsorbent (CS-MB) was stored in a desiccator for more usage, which is known as Chitosan-modified bentonite (CS-MB). The flow chart of Chitosan-Modified bentonite preparation is shown in Figure 2.

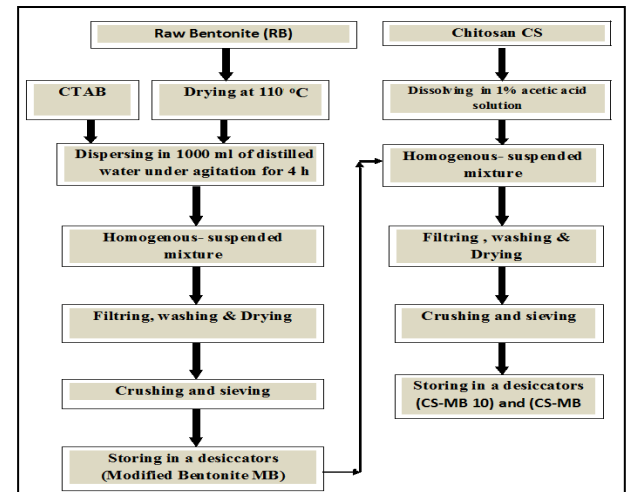


Fig. 2: Flowchart of Chitosan-Modified Bentonite.

2.4. Effect of adsorbent dosage

Different adsorbents in the adsorption of the crude oil (RB, MB, CS-MB10 and CS-MB30) were utilized to investigate the effect of adsorbent dosage. Different dosages of (400, 600, 800, 1000, 1200, 1400, and 1500mg) of each adsorbents were mixed with 50 ml of initial concentrations (500 mg/L of O/W emulsion). The initial pH of oily water was kept at 7. 1M of HCl and 1M of NaOH solutions are used to justify the pH of the solution. Then the solution was agitated at 180 RPM for 2 h approximately in a shaker water bath at 25°C. After 2 h of shaking, the solutions were filtered using vacuum pressure and filter paper. The residual concentration of crude oil in the filtrate solution was measured using TD500D™ Oil in Water Meter. Finally, select the best dosage of RB, MB, CS-MB10 and CS-MB30 at the highest efficiency of adsorption.

2.5. Effect of pH of the oily water solution

To obtain the best pH for crude oil adsorption onto each of adsorbents RB, MB, CS-MB10 and CS-MB30, series of batch experiments was studied by use of different pH value (2, 4, 6, 8, 10) for O/W solution. The best dosage of RB, MB, CS-MB10 and CS-MB30 was to be added to 50 ml with initial concentration of 100 mg/L of O/W solution. To adjust 1M solution of NaOH or HCl was used. Then the solution was placed in bottles that agitated at 180 RPM speed for about 2 h in a shaker water bath at 25°C. After 2 h of shaking the solutions were filtered by using vacuum pressure and filter paper. The filtered solution was analyzed for the remaining crude oil concentration by TD 500D™ Oil in Water Meter. The best pH of RB, MB, CS-MB10 and CS-MB30 was then selected at maximum remediation of crude oil.

2.6. Effect of contact time

In order to obtain the most excellent contact time for adsorption of crude oil onto different adsorbents RB, MB, CS-MB10 and CS-MB30 a series of experiments were achieved at different contact time (0.5, 1, 1.5, 2, 2.5, 3, 3.5, 4, 4.5 and 5h) with best of adsorbent dosages and the pH of adsorbate solutions. A 50 ml of O/W solution was placed in the bottles with best pH. The best dosage of each adsorbent MB, CS-MB10 and CS-MB30 were added to each bottle. The agitated for different times in a shaker water bath at 25°C and 180 rpm speed. Then filtered by using vacuum pressure and filter paper. The remaining concentration of crude oil in the filtrate solution was analyzed by using TD500D™ Oil in Water Meter. The best time of RB, MB, CS-MB10 and CS-MB30 was then selected at maximum adsorption efficiency.

2.7. Equilibrium isotherms

The equilibrium isotherms for adsorption of crude oil onto all the adsorbents RB, MB, CS-MB10 and CS-MB30 were performed experiments using the best adsorbent dosage, the best pH and the best adsorption period for each adsorbents. A 50 ml volume of O/W solution with different initial concentration (125, 250, 375, 500, 625 and 750 mg/L) was added to bottles containing of the optimum adsorbent amount and the pH of the solution. Then they are agitated for best time in a shaker water bath at 25°C and 180 RPM speed. The solutions were filtered by using vacuum pressure and filter paper. The remaining crude oil concentrations in the filtrate were determined by using TD500D™ Oil in Water Meter. The percentage sorption efficiency calculated using the following Eq. 1 [6]:

$$\% \text{ Sorption} = \frac{C_0 - C_e}{C_0} * 100 \quad (1)$$

The amount of adsorption at equilibrium, q_e (mg/g), is given by Eq. 2.

$$q_e = \frac{(C_0 - C_e)V}{m} \quad (2)$$

Where q_t (mg/g) is the amount of adsorption equilibrium, C_0 and C_e (mg/L) is the initial and equilibrium concentration of adsorbate respectively, V is the volume of the solution (L), and m is the mass of adsorbent in grams.

2.7.1. Langmuir isotherm

"The Langmuir isotherm assumes monolayer coverage of adsorbate to be occur over a homogenous adsorbent surface. Graphically, plateau characterizes the Langmuir isotherm. Therefore, a saturation point is reached at equilibrium, where no further adsorption can occur. Sorption is assumed to take place at that site" [7]. The Langmuir isotherm is represented in Eq. 3 [8]:

$$q_e = \frac{Q_0 * K_L * C_e}{1 + K_L * C_e} \quad (3)$$

Langmuir adsorption parameters can be determined by transforming the Langmuir Eq.3 into linear form [8].

$$\frac{1}{q_e} = \frac{1}{Q_0} + \frac{1}{(Q_0 * K_L * C_e)} \quad (4)$$

Where C_e is the equilibrium concentration of adsorbate (mg/L), q_e is the amount of metal adsorbed per gram of the adsorbent at equilibrium (mg/g), Q_0 is maximum monolayer coverage, capacity (mg/g), K_L is Langmuir isotherm constant (L/mg).

2.7.2. Freundlich isotherm

The Freundlich isotherm model is an empirical expression describing the exponential distribution of activity centers, characteristic of heterogeneous surface and infinite surface coverage [9]:

$$\text{Log } q_e = \text{log } K_F + \frac{1}{n} \text{log } C_e \quad (5)$$

"Where q_e the amount of the sorbed analyte per unit weight of the solid phase at equilibrium concentration. C_e , K_F the Freundlich constant related to the sorption capacity, while $1/n$ shows the sorption intensity" [9].

2.7.3. The tempkin isotherm

Tempkin, considered "the effects of some indirect adsorbate/adsorbate interactions on adsorption isotherms". The heat of adsorption in the layer of all molecules decreases linearly with the coverage due to these interactions. The Tempkin isotherm can be written in the following form:

$$q_e = \frac{RT}{b} (\ln A C_e) \quad (6)$$

By rewriting Eq. 6 in a linear expression leads to the formation as:

$$q_e = \frac{RT}{b} \ln A + \frac{RT}{b} \ln C_e \quad (7)$$

Where

$$B = \frac{RT}{b} \quad (8)$$

According to Eq. 7 the data of adsorption can be analyzed. Constants A and B can be determined from the plot of q_e vs. $\ln C_e$. The constant B is related to the heat of adsorption [10].

3. Results and discussions

3.1. Characterization of adsorbents by FTIR

The functional groups of a commercial Chitosan (New Delhi-110002, INDIA) were characterized using Fourier Transform Infrared Spectrophotometer (FTIR) (IRTracer-100, Shimadzu Co., Japan). FTIR analysis was carried out in the range from 4000-400 cm^{-1} as shown in (Figure 4). The absorption bands of Chitosan were similar to those of standard chitosan as shown in Table 2. The 3441-3417 cm^{-1} band could be assigned to (N-H), (O-H) and (NH_2) groups. This band was used in different amounts in Chitosan. The results are in agreement with (Zvezdova, 2010; Puspawati and Simpen, 2010). At band 1639 cm^{-1} (amide I, C=O stretching) and 1458 cm^{-1} (amide II, N-H bending), Chitosan exhibits characteristic absorption due to its amide groups [13]. The resulted bands at 1161 and 1091 cm^{-1} in Chitosan can be interpreted as a stretching vibration of C-O and C-O-C [14]. The peak at 898.83 and 702.097 cm^{-1} were due to ring stretching.

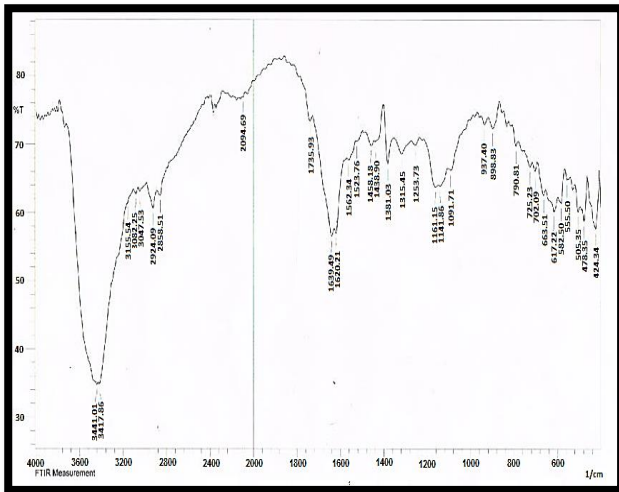


Fig. 4: FTIR of Commercial Chitosan.

Table 2: Functional Group of Commercial Chitosan Compared to Standard Chitosan [12]

Group	Wave length (cm ⁻¹)	
	Standard Chi-tosan	Commercial Chi-tosan
OH	3450	3441.01
N-H stretching	3335	3417.86
C-H stretching	2891.1	2858.51
NH ₂ Cutting N-H bending	1655	1639.49
CH ₃	1419.5	1458.18
C-O-C	1072.3	1091.71
NH ₂	850-750	898.83
N-H	715	702.09

Figure 5 shows the FTIR spectra of raw bentonite (RB). This figure shows a broad band's at 3425.58 cm⁻¹ and 1639.49 cm⁻¹ which may be resulted H-O-H stretching and H-O-H bending indicated the presence of an adsorbed water [15]. Further peaks can be seen at the band 1041.56 cm⁻¹, 528.50 cm⁻¹ and 420.48 cm⁻¹ due to the presence of Si-O stretching vibration, Si-O-Al and Si-O-Si bending vibrations, agree with the results of (Zheng et al., 2007; Xin et al., 2011).

The FTIR spectrum of Modified Bentonite (MB) by impregnation with cetyltrimethyl ammonium bromide (CTAB) is shown by Figure 6. The sharp bands at 2924.09 and 2850.79 cm⁻¹ correspond to the CH₂ asymmetric stretching mode and the symmetric stretching mode respectively. These two bands were not present in raw bentonite. The results indicated that the CTAB molecule was impregnated into the interlayer space of the bentonite as reported by (Guo et al., 2012). The increases in the intensity of the peak at 1469.76 cm⁻¹ in were compared to that of RB. The comparison indicates that the bending vibration of N-H is of secondary amines. These existed in the structure of CTAB, contains secondary amines before impregnation. Thus, it was expected that the CTAB impregnated clay contains this functional group. The results are in agreement with (Fosso-Kankeu et al., 2015). Broadband at 1022.27 cm⁻¹ represents Si-O-Si stretching vibrations. The shifts in Si-O-Si refer to an intercalation of CTAB into the interlayer space of the bentonite [20]. FTIR spectra of Chitosan-bentonite composite (CS-MB10 and CS-MB30) are shown in Figures 7 and 8 respectively. The presence of new bands at 1550.77 cm⁻¹ and 1543.05 cm⁻¹ in CS-MB10 and CS-MB30 were proportional to the NH₂ vibration mode of the Chitosan. "This indicates that the Chitosan molecules were introduced into the interlayer space of the bentonite structure" [18].

3.2. BET analysis of adsorbents surface area

The surface area of RB, MB, CS-MB10 and CS-MB30 were determined by the BET (model 9600, USA). In the present study, the surface area of raw bentonite (RB) and modified by cetyl-trimethylammonium bromide (MB) were measured as 71m²/g and

56m²/g respectively. A decrease in the surface area was observed for CTAB- bentonite. This is due to the fact that the nitrogen molecules cannot access the internal surface of CTAB- bentonite. The surface area decreased to (49 m²/g for CS-MB10 and 45 m²/g for CS-MB30) when the impregnation process was followed by modifying bentonite (MB) as shown in Table 3. In addition, it can be seen that the pore volume of CS-MB10 and CS-MB30 are higher than other adsorbents. This decrease in surface area of the adsorbents (CS- MB10 and CS- MB30) is ascribed to the creation of new pores resulting from impregnation process and the cross-linking. These results illustrate that the biocomposite adsorbents of biopolymer impregnated modified bentonite (CS-MB10 and CS-MB30) is successful adsorbent. These results is agreement with (Futalan et al., 2011; Guijuanet al., 2012).

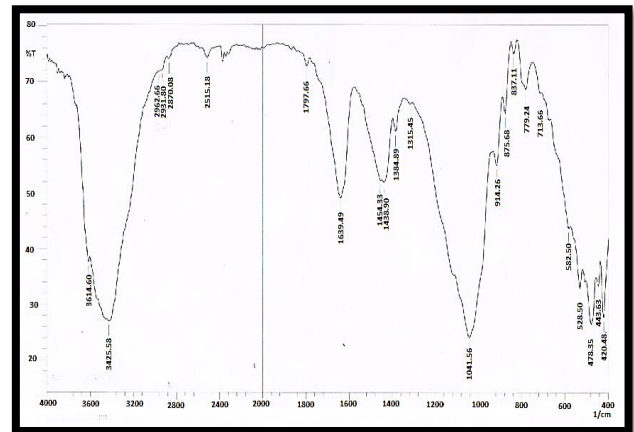


Fig. 5: FTIR of Raw Bentonite (RB).

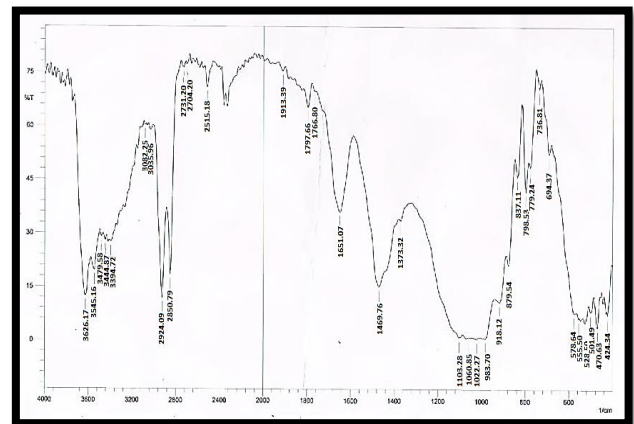


Fig. 6: FTIR of Modified Bentonite (MB).

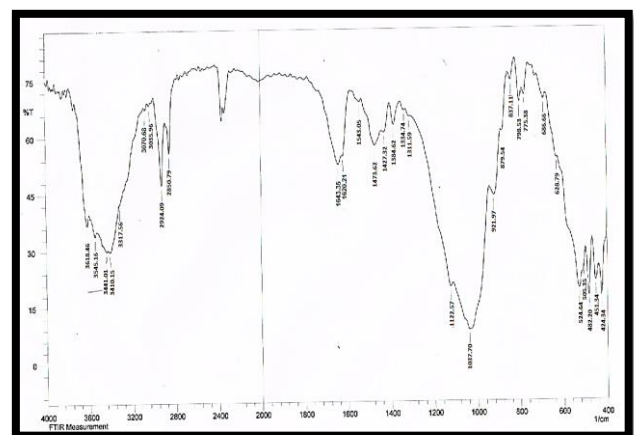


Fig. 7: FTIR of Chitosan- Modified Bentonite (CS-MB10%).

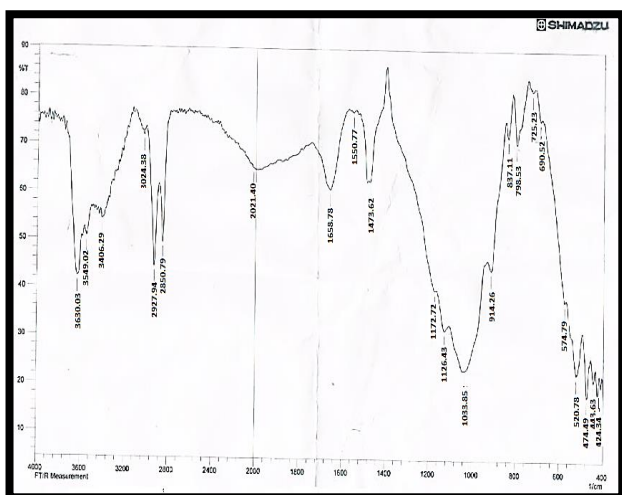


Fig. 8: FTIR of Chitosan- Modified Bentonite (CS-MB30%).

Table 3: Surface Area and Pore Volume Characterization of RB, MB, CS-MB10 and CS- MB30 Adsorbents by BET Analysis

Adsorbents	BET Surface Area (m ² /g)	Pore Volume (m ³ /g)
CH	4.15	∞∞∞∞∞
RB	71	0.124
MB	56	0.18254
CS-MB10	49	0.25488
CS-MB30	45	0.31125

3.3. Effect of adsorbents dosage on adsorption of crude oil

Figure 9 shows the effect of adsorbent dosage on the adsorption efficiencies for crude oil onto (RB, MB, CS-MB10 and CS-MB30) at 25°C and 500 mg.L⁻¹ initial concentrations. The adsorption efficiency of crude oil onto (RB and MB) increased with increasing the adsorbent dosage. It was varied from 19.877% and 29.7% to 73.5% and 90.2% respectively. When using (CS-MB10 and CS-MB30) as adsorbent materials, the adsorption efficiency varied from 40.3 % and 55.9 % to 93% and 97.5 % respectively. The adsorption process was noticed to be faster during the initial stages for all adsorbents. This may be due to the formation of new pores that provided more vacant adsorption sites to improve MB dye adsorption through the film around the adsorbent and onto pores of the CS-MB10 and CS-MB30 [23], [24]. Furthermore, the increase in RB and MB after 1400 mg has no significant effect on the removal efficiency due to the equilibrium state between the adsorbent (solid) and adsorbate (liquid). Conversely, the CS-MB10 and CS-MB30 reached the equilibrium state after 1200 mg. This is due to the fact that every adsorbent has a limited number of active binding sites which becomes with time harder to be occupied with the oil. Therefore, adsorbent dosage of 1200mg for every adsorbent of (CS-MB10 and CS-MB30) and 1400mg for (RB and MB) were chosen as the optimum dosage in order to obtain maximum adsorption efficiencies of oil. The obtained adsorption efficiencies were 90.81%, 95.85%, 72.46% and 89.08% respectively.

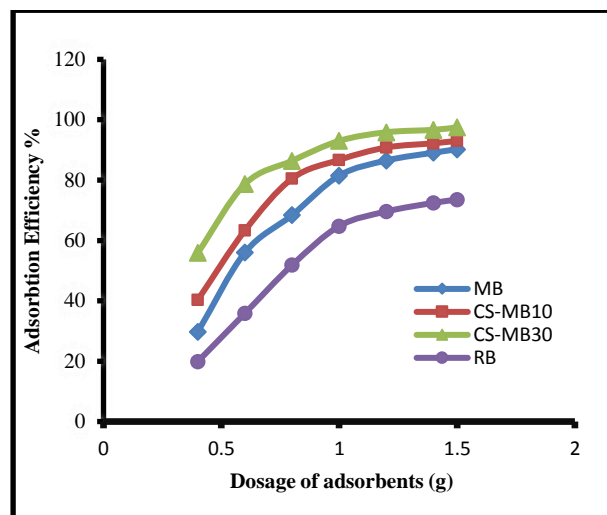


Fig. 9: The Effect of Adsorbent Dosage on the Adsorption Efficiency of Crude Oil onto Different Adsorbents (at C₀=500 Mg.L⁻¹, Ph 7.0, 2h, 180 RPM, and 25°C).

3.4. Effect of ph. solution on adsorption of crude oil

The pH effect of crude oil solution on the adsorption efficiencies of different types of adsorbents (RB, MB, CS-MB10 and CS-MB30) is shown in the Figure 10. These experiments were conducted at the optimum adsorbent dosages (1.4g for every RB and MB, and 1.2g for every CS-MB10 and CS-MB30) which added to 50ml of oily water solution at an initial concentration of 500mg.L⁻¹. The contents of the bottles were placed in bath shaker and agitated at 180 RPM for 2hours at 25°C. The pH of each sample was adjusted by adding 0.1 M HCl and 0.1 M NaOH. Figure 10 shows that the removal efficiencies of crude oil onto (RB, MB, CS-MB10 and CS-MB30) increased as the pH increases from 2 to 6 with the maximum removal efficiency at a pH value of 6. Whereas the removal efficiencies decreased at pH > 6. The adsorption efficiency varied from 54.45 %, 80.53 %, 81.77% and 83.46% to 72.34%, 89.79%, 91.02% and 91.99% for RB, MB, CS-MB10 and CS-MB30, respectively. The maximum obtained adsorption efficiencies were 72.34%, 89.79%, 91.02% and 91.99% at the pH 6.

The surface charge of bentonite is a strong function of the pH. MB adsorbent is better than RB and this may be related to that the quaternary ammonium attached to the clay surface and partially neutralized the negative charge of the bentonite. Therefore; due to the surfactant exchange the MB adsorbent became more hydrophobic and compared to the bentonite [26] (Emam, 2013). It was clear from the results that at pH =6 a higher adsorption efficiencies of oil onto composite adsorbents (CS-MB10 and CS-MB30) compared to the other adsorbents RB and MB. This behavior can be explained by the functional groups such as amino (-NH₂) group and the carboxylic (-COOH) group that formed on the surface of the composite adsorbent (CS-MB10 and CS-MB30). These functional groups provide various adsorption sites and increase the adsorption capacity of oil from oily water solution. These results demonstrated that the chitosan is successfully impregnated onto the surface of the modified bentonite. This leads to the formation of new porous structure in the composite adsorbents (CS-MB10 and CS-MB30). Therefore, the pH value of 6 was chosen as the optimum value of crude oil solution in order to obtain the maximum adsorption efficiencies of oil (72.34%, 89.79%, 91.02% and 91.99%) for each adsorbent of RB, MB, CS-MB10, and CS-MB30 respectively.

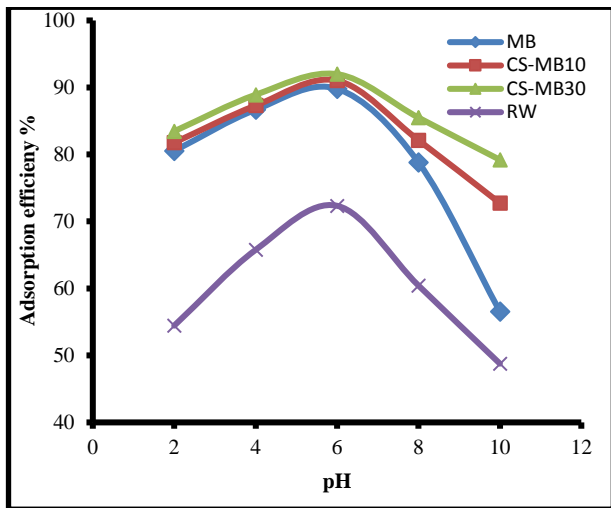


Fig. 10: The Initial Ph Effects of the Adsorption in the Crude Oil Solution for Different Adsorbents (at $C_o=500 \text{ Mg.L}^{-1}$, Dosage (1.4 G for RB and MB, 1.2 G for CS-MB10 and CS-MB30), 2 H, 180 RPM, and 25°C).

3.5. Effect of contact time on adsorption of crude oil

Figure 11 shows the effect of contact time on the adsorption efficiencies of crude oil onto different types of adsorbents (RB, MB, CS-MB10 and CS-MB30). The experiments were performed for time periods of (0.5, 1, 1.5, 2, 2.5, 3, 3.5, 4, 4.5, and 5 hours). It can be seen that the rate of crude oil adsorption increased sharply in the first 2 hours. Thereafter, the increase of adsorption rate tends to be slow and eventually reached equilibrium state between adsorbate (solute) and adsorbent (solid). The equilibrium state was reached after 3 hours. The maximum adsorption efficiency was 96.40% for CS-MB30. The adsorption efficiency, increasing quickly at the beginning of the process as the active binding sites onto the adsorbent surface increase too. Then the increases in the adsorption efficiency decreased with increasing the contact time. This decrease was due to a limited number of active binding sites, agree with (Emam, et al., 2013; Sokker, et al., 2011). Also, the remaining oil may be formed to block some porous surface structure. This means that the remaining oil is no longer diffuse into the active adsorption sites that present on the interior walls of adsorbent. Therefore, treatment time of 2 h was selected as the optimum treatment time for all adsorbents (RB, MB, CS-MB10, and CS-MB30) in order to obtain the maximum adsorption efficiencies of oil, that were 72.75%, 88.59%, 90.92% and 95.47% respectively.

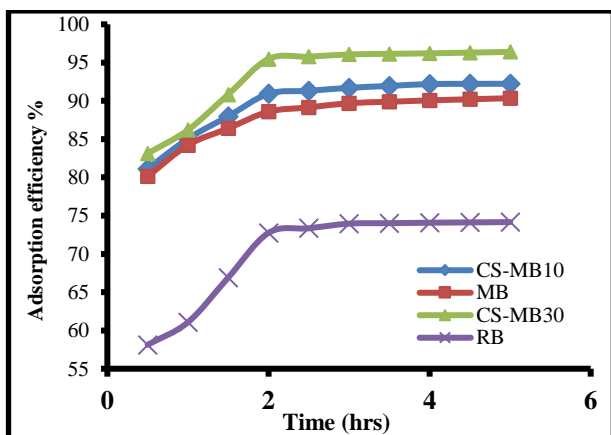


Fig. 11: Effect of Contact Time for Adsorption of Crude Oil onto Different Adsorbents (At $C_o=500\text{mg.L}^{-1}$, Ph 6.0, Dosage (1.4g for RB and MB, 1.2g for CS-MB10 and CS-MB30), 180 Rpm, and 25°C).

3.6. Equilibrium isotherm on adsorption of crude oil

The adsorption isotherm curves of crude oil onto each of adsorbents RB, MB, CS-MB10 and CS-MB30 were produced through plotting

adsorption capacity (mass of the oil adsorbed per unit mass of adsorbent) against the remaining concentration of the oil (C_e). The experimental data for crude oil adsorption onto different types of adsorbents (MB, RM, CS-MB10, and CS-MB30) are correlated with the three theoretical adsorption isotherm models (Langmuir, Freundlich and Temkin) as shown in Figures 12, 13, 14 and 15 respectively. The parameters of each model and adsorbent were listed in Table 4. Figures 12 and 13 show that the adsorption capacity of crude oil onto RB and MB was increased with the increase in the concentration of the solution. This behavior could be explained by the strong surface interaction between oil and adsorbents [26]. Based on the correlation coefficients R^2 listed in Table 4, it can be seen that the Temkine isotherm has a higher fit to the experimental data more than the Freundlich and Langmuir adsorption isotherm models for CS-MB10. In addition, The best fit of the experimental for CS-MB30 data occurs in the the Langmuir isotherm model compared to the Freundlich and Temkine adsorption isotherm models. The comparison in higher adsorption capacity of MB and RB are clarified by the way that the intercalation of organic action builds the surface sites accessible for adsorption. "The modification increases the positive charges on the surface and it facilitates the attraction towards crude oil" [27].

The correlation coefficients (R^2) listed in Table 4 indicted that the results will be best fit in experimental data by Temkin and Langmuire adsorption isotherm for RB and MB respectively.

The adsorption capacity of crude oil onto CS-MB10 and CS-MB30 increases with the increase of the oil concentration in the solution as shown in Figures 14 and 15. This behavior can be explained as a result of the presence of the functional groups of the adsorbents surface such as amine and hydroxide which enhanced the adsorption capacity of adsorbents surface. The desirable chemical binding, such as electrostatic attraction can occur between crude oil and chitosan [28]. Thereafter, the active adsorption sites were occupied and the concentration of remaining oil is decreased until equilibrium state is obtained.

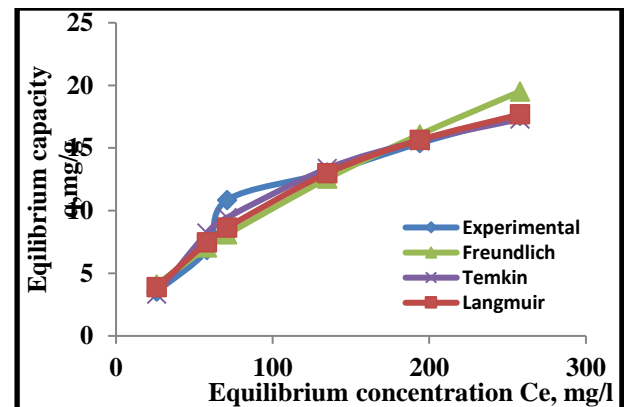


Fig. 12: Experimental and Theoretical Models of Adsorption Isotherms for the Crude Oil in RB (at 25°C , 1.4 G, 3hrs. in addition, Ph 6).

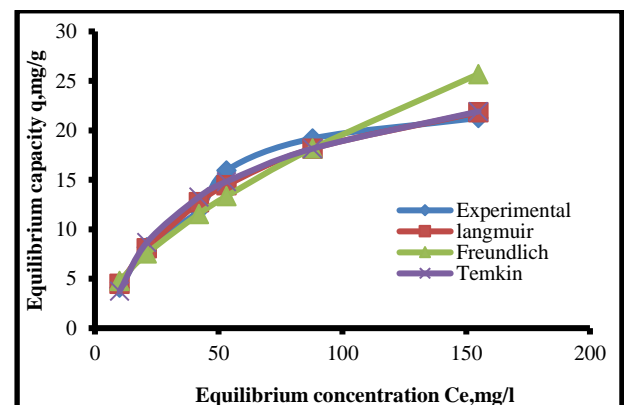


Fig. 13: Experimental and Theoretical Models of Adsorption Isotherms for the Crude Oil in MB (at 25°C , 1.4 G, 3 H, and Ph 6).

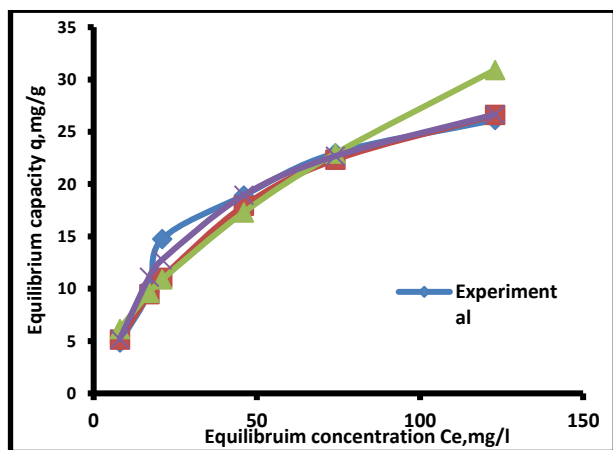


Fig. 14: Experimental and Theoretical Models of Adsorption Isotherms for the Crude Oil in CS-MB10 at (25 °C, 1.4 G, 3h, and Ph 6).

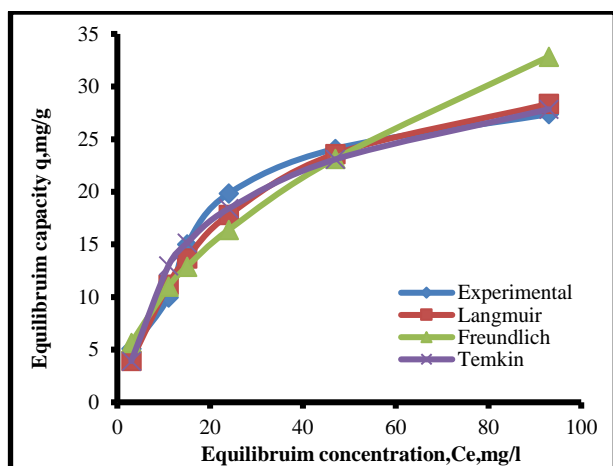


Fig. 15: Experimental and Theoretical Models of Adsorption Isotherms for the Crude Oil in CS-MB30 at (25°C, 1.4 G, 3h, and Ph 6).

Table 4: The Isotherm Constants of Langmuir, Freundlich and Temkin for Crude Oil Remediation onto RB, MB, CS-MB10 and CS-MB30 Adsorbents at 25 °C

Model	Parameters	RB	MB	CS-MB10	CS-MB30
Langmuir Eq.(2.3& 2.4)	q_m (mg/g)	29,2604	29,7719	27,4032	35,7143
	b (l/mg)	0.0059	0,1177	0,1199	0,0414
	R^2	0,9240	0,9800	0,9700	0,9778
Freundlich Eq.(2.5)	$1/n$	0,7698	0,7128	0,0899	0.5132
	K_f	0,4477	1,1684	1,8084	2,2077
	R^2	0,9224	0,9476	0,907	0,942
Temkin Eq. (2.6)	A_T (L/g)	0,774	0,1763	0,2418	0,0841
	b_T	4,70	374	310,2	300,0
	B (J/mole)	7,0901	7,7226	7,808	7,9796

4. Conclusions

In the present work, the bioadsorption of crude oil from aqueous solution onto different adsorbents such as RB, MB, CS-MB10 and CS-MB30, lead to the following conclusions: 1) Iraqi bentonite (RB) is a cheap and effective adsorbent and can be successfully used for removing of crude oil from wastewater. 2) Natural biopolymer "Chitosan" treated with modified bentonite by impregnation was used as biocomposite adsorbent for the removal of crude oil from aqueous solution. 3) The batch adsorption of crude oil increased with the increase in adsorbent dosage until equilibrium is reached. The maximum adsorption efficiency of crude oil at 1.4g was found to be 72.46% for RB, 89.09% for MB and at 1.2g was found to be 90.81 % for CS-MB10 and 95.85 % for CS-MB30. 4) The maximum adsorption efficiency was obtained at pH 6 for removal of crude oil onto each RB, MB, CS-MB10 and CS-MB30 at 25 °C. 5) The crude oil adsorption increased with the increase in contact time until an equilibrium state was reached. Best contact

time was selected at 2 hours with the maximum adsorption efficiency of crude oil onto each of RB, MB, CS-MB10 and CS-MB30. 6)

The results indicate that Temkin isotherm fits the experimental data better than Freundlich and Langmuir adsorption isotherm for RB and CS-MB10. The Langmuir isotherm fit the experimental data better than Freundlich and Temkin adsorption isotherm for MB and CS-MB30.

References

- [1] Ahmad A.L., Sumathi S. and Hameed B.H., Residual oil and suspended solid removal using natural adsorbents chitosan, bentonite and activated carbon: A comparative study, *Chemical Engineering Journal*, 108, (2005) 179–185. <https://doi.org/10.1016/j.cej.2005.01.016>.
- [2] Sirotkina E. E. and Novoselova L.YU., Materials for Adsorption Purification of Water from Petroleum and Oil Products, *Chemistry for Sustainable Development*, 13 (2005) 359–375.
- [3] Cheryan M. and Rajagopalan N., Membrane processing of oily streams Wastewater treatment and waste reduction, *Journal of Membrane Science*, 151(1998) 13-28.
- [4] Babel S. and Kurniawan T. A., Low-cost adsorbents for heavy metals uptake from contaminated water: a review, *Journal of Hazardous Materials*, (2003) 219–243. [https://doi.org/10.1016/S0304-3894\(02\)00263-7](https://doi.org/10.1016/S0304-3894(02)00263-7).
- [5] Juang R.S., Lin S.H., Tsao K.H., Mechanism of Sorption of Phenols from aqueous solutions onto surfactant-modified montmorillonite, *Journal Colloid Interface Science*, 2 (2002) 234– 254. <https://doi.org/10.1006/jcis.2002.8629>.
- [6] Horzum N., Boyacı E., Eroglu A. E., Shahwan T. and Demir M. M., Sorption Efficiency of Chitosan Nanofibers toward Metal Ions at Low Concentrations, *Journal of Hazardous Materials*, 164 (2009) 675–682.
- [7] Ali Hosseini A., Taghikhani V., Safekordi A.A. and Bastinado. Correlation of the equilibrium sorption of crude oil by expanded perlite using different adsorption isotherms at 298.15 k, *Int. J. Environ. Sci. Tech.*, 7, 3 (2010) 591-598. <https://doi.org/10.1007/BF03326168>.
- [8] Dada A.O., Olalekan A.P., Olatunya A.M. and Dada O., (2012), Langmuir, Freundlich, Temkin and Dubinin–Radushkevich, Isotherms Studies of Equilibrium Sorption of Zn²⁺ Unto Phosphoric Acid Modified Rice Husk, *Journal of Applied Chemistry*, 3, (2012) 38-45.
- [9] Qureshi I., Memon S. and Yilmaz M., Estimation of chromium(VI) sorption efficiency of novel regenerable p-tert butylcalix[8]areneoctamide impregnated Amberlite resin, *Journal of Hazardous Materials*, 164 (2009) 675–682. <https://doi.org/10.1016/j.jhazmat.2008.08.076>.
- [10] Allen S.J., Mckay G. and Porter J.F., Adsorption isotherm models for basic dye adsorption by peat in single and binary component systems, *Journal of Colloid and Interface Science*, 280 (2004) 322–333. <https://doi.org/10.1016/j.jcis.2004.08.078>.
- [11] Zvezdova D., (2010), Synthesis and characterization of chitosan from marine sources in Black Sea, *Scientific work of the Russian university*, 49 (2010) 65-69.
- [12] Puspawati N. M. and Simpen I N., Optimasi deasetilasi khitin dari kulit udang dan cangkang kepiting limbah restoran seafood menjadi khitosan melalui variasi konsentrasi naoh, *jurnal kimia*, 4, (2010) 79-90.
- [13] Don T-M., King C-F., Chiu W-Y and Peng C-A , (2006), Preparation and characterization of chitosan-g-poly (vinyl alcohol)/poly(vinyl alcohol) blends used for the evaluation of blood-contacting compatibility, *Carbohydrate Polymers*, 63 (2006) 331–339.
- [14] Jagtap S., Thakre D., Wanjari S., Kamble S., Labhsetwar N. and Rayalu S., (2009), New modified chitosan-based adsorbent for de-fluoridation of water, *Journal of Colloid and Interface Science*, 332 (2009) 280–290. <https://doi.org/10.1016/j.jcis.2008.11.080>.
- [15] Anirudhan T.S. and Ramachandran M., (2006), Adsorptive removal of tannin from aqueous solutions by cationic surfactant-modified bentonite clay, *Journal of Colloid and Interface Science*, 299 (2006) 116–124. <https://doi.org/10.1016/j.jcis.2006.01.056>.
- [16] Zheng L., Xu S., Peng Y., Wang J. In addition, Peng G., (2007), Preparation and swelling behavior of amphoteric superabsorbent composite with semi-IPN composed of poly (acrylic acid)/Ca-bentonite/poly (dimethyldiallylammonium chloride), *Polymer. Advanced Technologies*, 18 (2007) 194–199. <https://doi.org/10.1002/pat.850>.

- [17] Xin X., Si W., Yao Z., Feng R., Dua B., Yan L. and Wei Q. , (2011), Adsorption of benzoic acid from aqueous solution by three kinds of modified bentonites, *Journal of Colloid and Interface Science*, 359 (2011) 499–504. <https://doi.org/10.1016/j.jcis.2011.04.044>.
- [18] Guo J., Chen S., Liu L., Li B., Yang P., Zhang L and Feng Y., (2012), Adsorption of dye from wastewater using chitosan–CTAB modified bentonites *Journal of Colloid and Interface Science*, 382 (2012) 61–66. <https://doi.org/10.1016/j.jcis.2012.05.044>.
- [19] Fosso-Kankeu E., Waanders F., and Fourie C. L., (2015), Surfactant Impregnated Bentonite Clay for the Adsorption of Anionic Dyes, 7th International Conference on Latest Trends in Engineering & Technology (ICLTET), 2015. <https://www.researchgate.net/publication/286019223>.
- [20] Huang J., Wanga X. B., Jina Q., Liua Y. and Wangb Y., (2007), Removal of phenol from aqueous solution by adsorption onto OTMAC-modified attapulgite, *Journal of Environmental Management*, 84 (2007) 229–236. <https://doi.org/10.1016/j.jenvman.2006.05.007>.
- [21] Futralan C. M., Kan C-C., Dalidac M. L., Hsien K-J., Pascud C. and Wanb M-W, (2011), Comparative and competitive adsorption of copper, lead and nickel using chitosan immobilized on bentonite, *Carbohydrate Polymers*, 83 (2011) 528–536 <https://doi.org/10.1016/j.carbpol.2010.08.013>.
- [22] Guijuan J., Weieei B., guimi G., Baichao A., Haifeng Z. and shucai G., (2012), Removal of Cu(II) from aqueous solution using a novel crosslinked Alumina-Chitosan hybrid adsorbent, *Chinese J. of chem. Eng.*, 20, 4 (2012) 641–648. [https://doi.org/10.1016/S1004-9541\(11\)60229-2](https://doi.org/10.1016/S1004-9541(11)60229-2).
- [23] Sokker H.H., El-sawy N.M., Hassan M.A., and El-anadouli B.E., (2011), Adsorption of crude oil from aqueous solution by hydrogel of chitosan based polyacrylamide prepared by radiation induced graft polymerization, *J. Hazard. Mater.* 190, (2011) 359–365. <https://doi.org/10.1016/j.jhazmat.2011.03.055>.
- [24] Ahmad A.L., Sumathi S. and Hameed B.H., (2005), Adsorption of residue oil from palm oil mill effluent using powder and flake chitosan: Equilibrium and kinetic studies *Water Research*, 39 (2005) 2483–2494. <https://doi.org/10.1016/j.watres.2005.03.035>.
- [25] Emam E.A., (2013), Modified Activated Carbon and Bentonite Used to Adsorb Petroleum Hydrocarbons Emulsified in Aqueous Solution, *American Journal of Environmental Protection*, 2, 6 (2013) 161–169.
- [26] Yarkandi N. H., (2014), Removal of lead (II) from wastewater by adsorption, *Int. J.Curr. Microbiol. App. Sci*, 3, 4 (2014) 207–228.
- [27] Teofilovic V., Pavlicevic J., Bera O., Jovicic M., Budinski-Simendic J., Szécsényi K. M. and Aroguz A., (2014), the preparation and thermal properties of chitosan/bentonite composite beads, *Hem. Ind.*, 68, 6 (2014) 653–659. <https://doi.org/10.2298/HEMIND130905088T>.
- [28] Maghsoodloo Sh., Noroozi B., Haghi A.K. and Sorial G.A., (2011), Consequence of chitosan treating on the adsorption of humic acid by granular activated carbon, *Journal of Hazardous Materials*, 191(2011) 380–387. <https://doi.org/10.1016/j.jhazmat.2011.04.096>.